



Contents lists available at ScienceDirect

Arabian Journal of Chemistry

journal homepage: www.ksu.edu.sa

L-histidine doped CDs from *Zingiber Montanum* using hydrothermal method to enhance its antimicrobial activity and imply for latent fingerprint detection

David Nugroho^a, Aphinya Thinthasit^a, Indra Memdi Khoris^{b,1}, Pooncharat Siriputthaiwan^c, Rachadaporn Benchawattananon^{a,*}, Saksit Chanthai^{d,*}

^a Department of Integrated Science, Faculty of Science, Khon Kaen University, Khon Kaen 40002, Thailand

^b Research Institute of Green Science and Technology, Shizuoka University, 836, Japan

^c Department of Microbiology, Faculty of Science, Khon Kaen University, Khon Kaen 40002, Thailand

^d Materials Chemistry Research Center, Department of Chemistry and Center of Excellence for Innovation in Chemistry, Faculty of Science, Khon Kaen University, Khon Kaen 40002, Thailand

ARTICLE INFO

Keywords:

Zingiber Montanum
Plant extract
Carbon dots
Forensic Science
Antibacterial activity

ABSTRACT

Carbon dots (CDs) from *Zingiber Montanum* as a natural resource were prepared and tested as an antimicrobial activity with various types of bacteria. Then nitrogen doped carbon dots (N-CDs) were subject to obtain from the plant extract doped with L-histidine using hydrothermal method, indicating their N-CDs fluorescence intensity increases, and can be visualized more brightness under UV lamp compared with its bare CDs. Besides its antimicrobial purpose, fingerprint image is utmost known as one of the important characteristics of the crime evident, in this study, the N-CDs are then aimed to apply on various non-porous material surfaces for latent fingerprint detection. It was shown that the fine powder of N-CDs mixed with starch give more detailed minutiae compared with that from black commercial powder. The applicable fingerprint tracer using this N-CDs/starch powder shows a bit long time clear results until 90 days, indicating that the new N-CDs developed enhances much more the fingerprint performance than its usual. In addition, to confirm the antimicrobial activity the N-CDs alone were also used for such antimicrobial testing via agarose disk diffusion assay against both gram negative and gram-positive bacteria, resulted satisfactorily that this nanomaterial can be a high potential use for antibacterial activity.

1. Introduction

Bacterial infections, especially by drug-resistant bacteria, have been a severe worldwide problem (Vallianou et al., 2019; Allianou et al., 2019). The efficacy of treating this infection is progressively diminishing as a result of escalating medication resistance caused by the improper utilization of antibiotics by individuals lacking comprehension of the prescribed guidelines for drug administration. (Hoozemans et al., 2021; Oldock et al., 2018; Ghobashy and Khafaga, 2017; Abdel Maksoud et al., 2022; Alshangiti et al., 2019; Ghobashy and Elhady, 2017). It is of urgent concern to develop alternative antimicrobial agents with excellent properties against bacterial infections. Recently, several nanomaterial compounds involving metals or metal oxides have aroused widespread

interest because of their great potential in the treatment of bacterial infections of antibiotic-resistant bacteria. The most common commensal inhabitant of the digestive systems of people and warm-blooded animals, *E. coli* is also one of the most significant pathogens. It belongs to the bacterial family Enterobacteriaceae. The organism in question exists as a commensal, engaging in a symbiotic relationship with its hosts that is mutually advantageous, while exhibiting a low propensity for causing pathogenic effects. However, it is also noteworthy that this particular microorganism is widely prevalent among both humans and animals, serving as a causative agent for a diverse range of diseases. *E. coli* is a significant host organism in biotechnology due to its unique traits, which include simplicity of handling, accessibility to the whole genome sequence, and capacity to grow in both aerobic and anaerobic

* Corresponding authors.

E-mail addresses: rachadaporn@kku.ac.th (R. Benchawattananon), sakcha2@kku.ac.th (S. Chanthai).

¹ Current Address: National Institute of Advanced Industrial Science and Technology, Tsukuba, Ibaraki 305-8565, Japan.

Table 1
Carbon dots preparation and their applications from various precursors.

Source of CDs	Synthesis Condition	Particle Size	Application of CDs	Reference
Sodium alginate	1100 W, 8 min	5 nm	Toughening agent	(Ganguly et al., 2020)
Watermelon peel	220 °C, 2 h	2 nm	Optical imaging	(Hu et al., 2020)
Table sugar	120 °C, 3 min	4 nm	Green reducing agent	(Lu et al., 2016)
Beetroot	180 °C, 10 h	5 nm	Pb ²⁺ detection	(Xu et al., 2015)
Green tea leave	350 °C, 2 h	2 nm	Optical imaging	(Naik et al., 2020)
Orange	120 °C, 150 min	1.5 nm	Biolabeling and optoelectronics	(Alam et al., 2015)
Aloevera	180 °C, 11 h	5 nm	Detection of tetrazine in food samples	(Dager et al., 2019)
Orange pericarp	100 °C, 5 h	2.9 nm	Nano biotechnology	(Ye et al., 2017)
Cabbage	140 °C, 5 h	2–6 nm	Bioimaging	(Roshni and Ottoor, 2015)
Coconut	180 °C, 4 h	12.9 nm	Fingerprint	(Nugroho et al., 2022)
<i>Andrographis paniculate</i>	160 °C, 8 h	2 nm	Cell Imaging	(Naik et al., 2020)
Citric acid & 1,2-ethylenediamine	720 W, 2 min	–	Iodide detection	(Du et al., 2013)
<i>Magnolia Grandiflora</i>	1400 W, 20 min	4 nm	Fingerprint	(Nugroho et al., 2022)
<i>Zingiber officinale</i>	180 °C, 1 h	2.3 nm	Accelerates wound healing	(Li et al., 2023)
<i>Zingiber officinale Rosc</i>	300 °C, 2 h	4 nm	Exhibiting efficient inhibition of human hepatocellular carcinoma cells	(Li et al., 2014)
O-phenylenediamine, D-Glu	200 °C, 3 h	2 nm	Antibacterial	(Qie et al., 2022)
levofloxacin	250 °C, 4 h	12.7 nm	Antibacterial	(Liang et al., 2021)
<i>Zingiber Montanum</i>	180 °C, 4 h	4 nm	Fingerprint & Antibacterial	This work

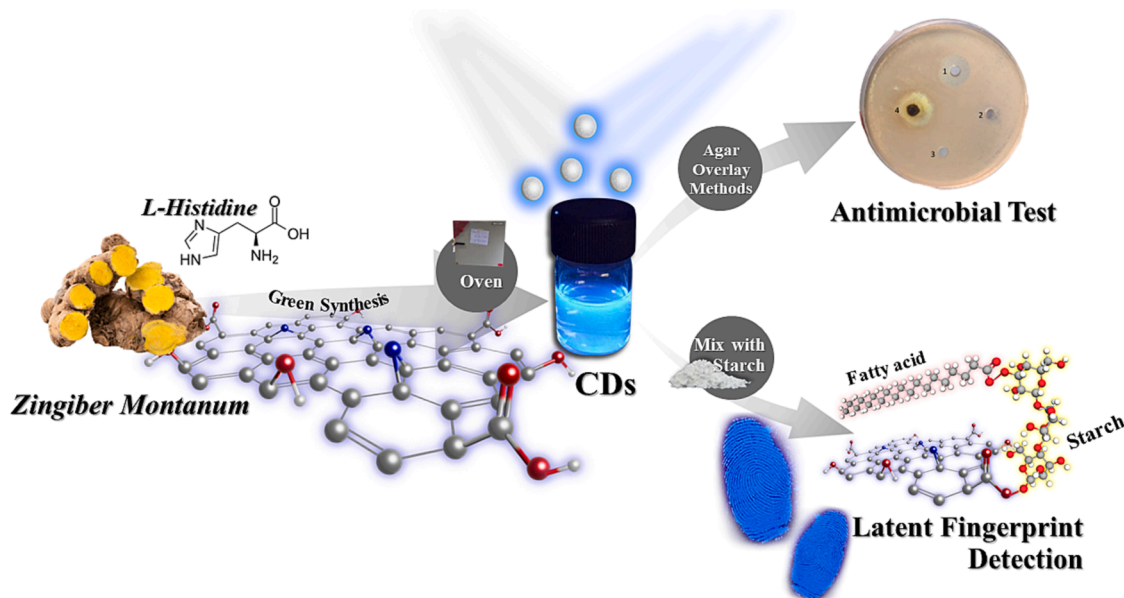


Fig. 1. Graphical abstract for the synthesis of N-CDs and their applications.

conditions. *Escherichia coli* (*E. coli*) is extensively employed in diverse applications within the industrial and medical sectors, making it the most commonly utilized microorganism in the realm of recombinant DNA technology (Kaper et al., 2004; Bilinski et al., 2012). *Serratia marcescens*, a bacterium characterized by its rod-shaped morphology and Gram-negative cell wall structure, belongs to the Enterobacteriaceae family. It exhibits a broad distribution across various ecological habitats, including water, soil, plant and insect life, and food sources. *Serratia marcescens* has the capability to synthesize several secondary metabolites of significant value, including prodigiosin, althiomycin, serratamolide, acetoin, and 2,3-butanediol (Williamson et al., 2006; Gerc et al., 2014; Rao et al., 2012). A rod-shaped, Gram-positive, primarily aerobic, spore-forming bacteria called *Bacillus megaterium* can be found in a wide variety of settings (Tang et al., 2019; Bramhanwade et al., 2016). However, it is important to balance antibacterial efficiency and biosafety, which has been constraints in the clinical application of these semiconductor nanomaterials, nanomaterial compounds such as graphene oxide, graphene, and carbon quantum dots have demonstrated efficient antimicrobial activity and high biocompatibility in their applications against several bacteria (Srivastava et al., 2016; Jayan et al., 2021; Kaur et al., 2020). Therefore, this carbon-based nanomaterial can

potentially be antibacterial material that can eliminate various bacterial infections with low cytotoxicity and excellent biocompatibility.

Fingerprint detection is essential for crime scene investigations and the examination of evidence because Fingerprints are valuable for personal identification. However, since the majority of fingerprints left at crime scenes are latent, detecting them becomes one of the largest obstacles for detectives looking for a perpetrator. The current methods still have issues, despite significant efforts to develop a unique detection methodology for identification (Fàbrega et al., 2018; Jiao et al., 2018; Koutsogiannis et al., 2020; Choi et al., 2018; Wang et al., 2017; Zhang et al., 2018; Macairan et al., 2019). These issues, such as low sensitivity, low selectivity, and interference from dark or patterned backgrounds, demand ongoing investigation. Latent fingerprint as one of important evidence in the crime cases because it can determine who the perpetrators are in a crime case, the residue that is left on the goods at the scene is produced from fat produced from the fat glands on human fingers to create fingerprints everyone is different and only specific to certain people (Yang et al., 2019; Chen et al., 2019; Diao et al., 2018; Bhalla et al., 2016; Wang et al., 2019; Nugroho et al., 2022; Liu et al., 2019; Liu et al., 2017).

Zingiber Montanum is a type of natural herbal plant that has high

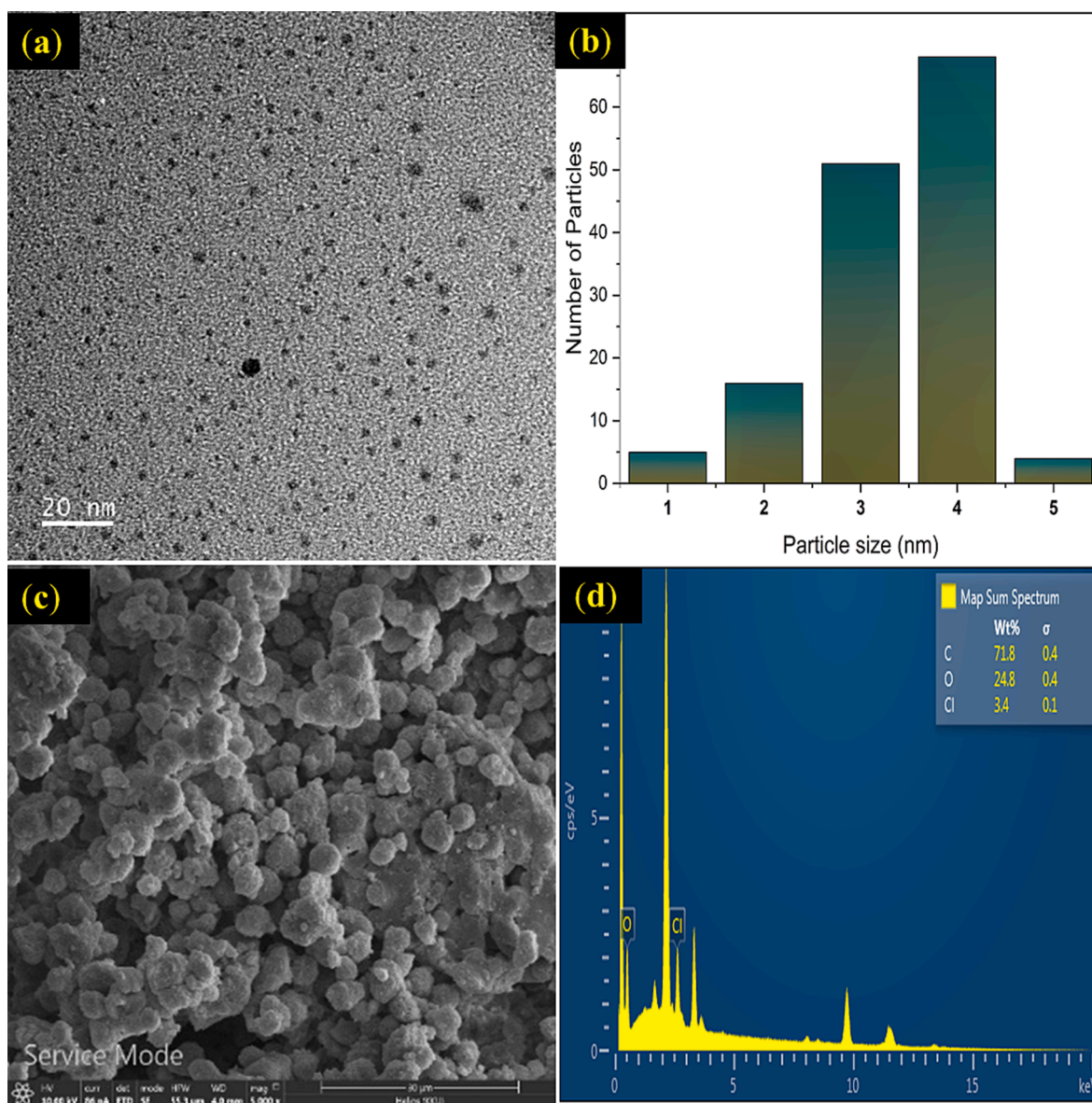


Fig. 2. Transmission electron microscope (TEM) of N-CDs (a). Histogram graph TEM of N-CDs (b), N-CDs/starch powder (c), and Energy dispersive X-ray (EDX) spectrum of N-CDs (d).

potential medicinal plant as an anticancer, anti-inflammatory, anti-fungal, antioxidant, anti-allergic and antibacterial, due to the natural ingredients it contains such as Zerembone, Curcumin, etc. Carbon dots (CDs) are tiny particles of carbon that have a size ranging from a few nanometers. They are typically synthesized from various carbon sources such as graphite, graphene, or carbon nanotubes, and have unique optical, electrical, and chemical properties that make them attractive for a wide range of applications. One of the main features of carbon dots is their ability to fluoresce with the general structure of CDs is sp^3/sp^2 , or emit light, when excited by an external energy source such as ultraviolet (UV) light. This property is due to the presence of defects or impurities in the carbon lattice structure, which can trap and release energy in the form of light. Carbon dots have a strong and stable fluorescence emission, which makes them attractive for use in imaging and sensing applications (Nugroho et al., 2023; Ganguly et al., 2020; Luo et al., 2020; Li et al., 2018; Chen et al., 2017; Liu et al., 2018; Hashemi and Mousazadeh, 2021; Hu et al., 2020). In addition to their fluorescence properties, carbon dots also have good chemical stability and biocompatibility, which makes them suitable for use in biomedical applications such as drug delivery and tissue engineering. They also have good electrical

conductivity, which makes them useful in electronics and energy storage applications (Xu et al., 2015; Alam et al., 2015; Dager et al., 2019; Ye et al., 2017; Nugroho et al., 2022; Roshni and Ottoor, 2015; Du et al., 2013; Yong et al., 2009; Yang et al., 2019). CDs synthesis can be carried out through the green synthesis pathway using natural materials, such as various types of flowers, lemon juice, coconut water, etc., the two ways to carry out CDs synthesis are bottom-up and top-down, Top-down process by breaking the big carbon bonds to be small segments using laser ablation and chemical oxidation, etc. In the bottom-up synthesis of carbon precursors using methods such as thermal pyrolysis, and microwaves (Chandrajith and Marapana, 2018; Djunaidi, 2020; Naik et al., 2020; Du et al., 2015; Yang et al., 2011; Guan et al., 2014; Lu et al., 2016; Sahu et al., 2012). There are several applications of carbon dots from including from zingiber family in the previous research such as wound healing, inhibition of human hepatocellular carcinoma cells, etc. (Table 1) In this study, the N-CDs has been prepared from *Zingiber Montanum* combined with L-histidine using hydrothermal method. Spectroscopic characteristics and morphology image analysis were conducted in detail. Also, novel data gave excellent inhibitory effects, expressed as its inhibition zone, on *E. coli* and *S. marcescens*, (gram-

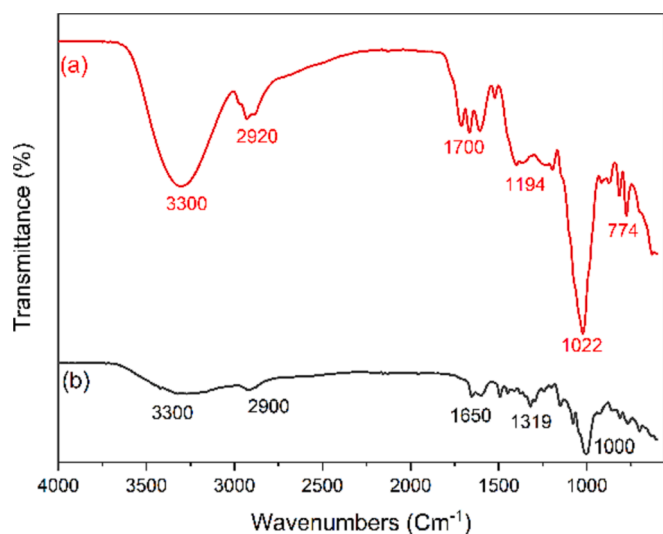


Fig. 3. Fourier transform infrared spectroscopy (FTIR) of (a) Carbon dots (CDs) and (b) N-Doped Carbon dots (N-CDs).

negative bacteria) and *B. megaterium* and *S. aureus*, (gram-positive bacteria). Their antibacterial mechanism of the N-CDs would be attributed to electrostatic interactions between the surface charge of N-CDs and bacterial cell walls (Fig. 1).

2. Materials and methods

2.1. Plant and chemicals

Zingiber Montanum plant was taken from the Faculty of Science flower park during summer season (March to June 2022), Khon Kaen University (Khon Kaen, Thailand). L-Histidine was purchased from Sigma Aldrich (USA). Ethanol was purchased from RCI Labscan, Thailand. Nutrient agar was purchased from HIMEDIA (India). Commercial tapioca powder (Five Stars brand) was from Kieng Supermarket, Khon Kaen. Black commercial fingerprint powder for police mate finger

palm food and pink ink powder from KAGAKU SOBI LTD, Japan. Commercial amoxicillin was obtained from the drug store, Khon Kaen University Student Complex I, Khon Kaen University.

2.2. Instruments

The synthesis of carbon dots (CDs) was conducted using hydrothermal technique within a heating oven (BINDER ED 115UL-120 V). The fingerprint mixture containing commercial tapioca powder was subject to centrifugation using the NF 800 centrifuge and stirred using the Daihan Scientific MSH-20D magnetic stirrer. The CDs product has been undergone various analytical techniques to assess its properties. These techniques include optical analysis using a commercial UV lamp at a wavelength of 365 nm, fluorescence and UV-visible spectrophotometry, X-ray photoelectron spectroscopy using KRATOS AXIS SUPRA, Fourier Transform infrared spectroscopy (FTIR) using Bruker TENSOR 27, energy-dispersive X-ray spectroscopy (EDX) using Oxford Instruments X-Maxn, focused ion beam, and for CHNS analysis using Thermo Scientific Flash 2000 N/Protein analyzer.

2.3. Synthesis of carbon dots (CDs) and L-histidine doped carbon dots (N-CDs)

Carbon dots has been synthesis by used one gram of *Zingiber Montanum* powder were added in 20 mL DI water, and then one-pot synthesized using hydrothermal method with various times (2, 4, 6 and 8 h) and temperatures (120, 140, 160 and 180 °C) working conditions. After synthesis, the N-CDs was filtered using a nylon filter membrane 0.22 μm and centrifuged at 10,000 × g rpm for 15 min. after get the optimum condition the N-CDs was been synthesis by One gram of *Zingiber Montanum* powder and 0.1 g L-histidine powder were added in 20 mL DI

Table 2
CHN elemental analysis of CDs and N-CDs.

Sample	N%	C%	H%
CDs	ND	88.13	11.87
N-CDs	5.49	75.49	19.02

Note: ND = not detectable.

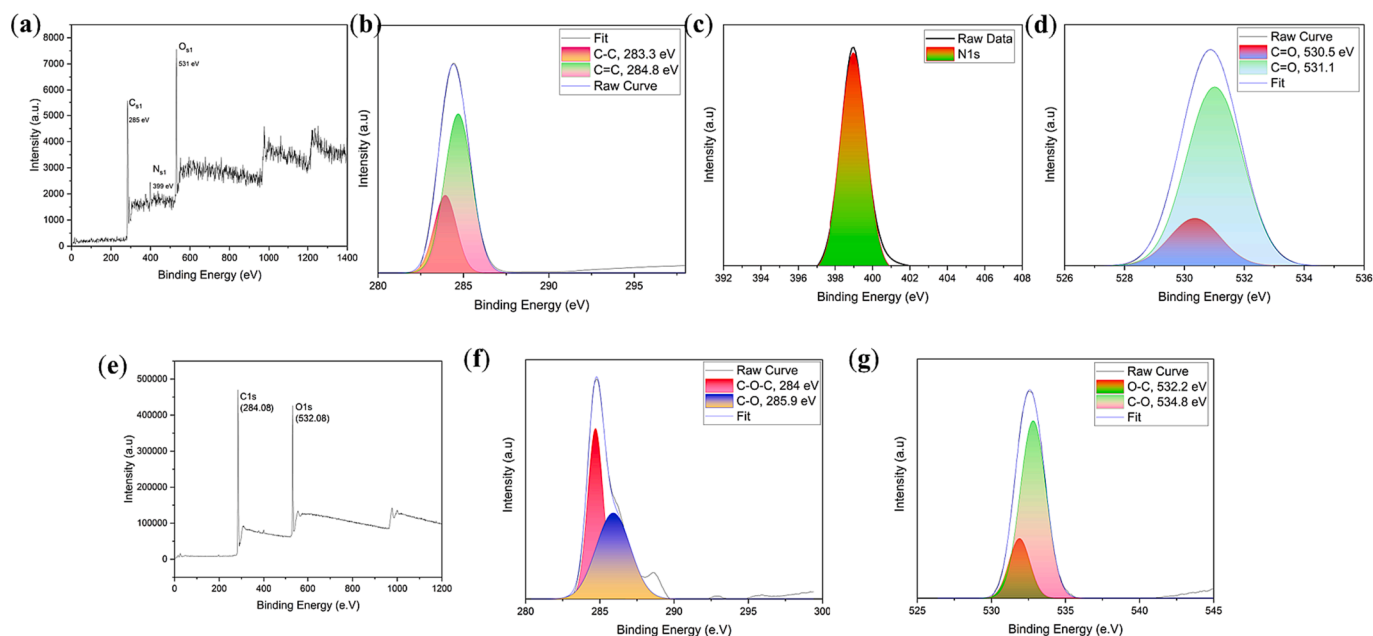


Fig. 4. X-ray photoelectron spectroscopy (XPS) spectra of N-CDs (a) and high-resolution XPS spectra of C_{1s} (b), N_{1s} (c), and O_{1s} (d). X-ray photoelectron spectroscopy (XPS) spectra of CDs (e) and high-resolution XPS spectra of C_{1s} (f), and C_{1s} (g).

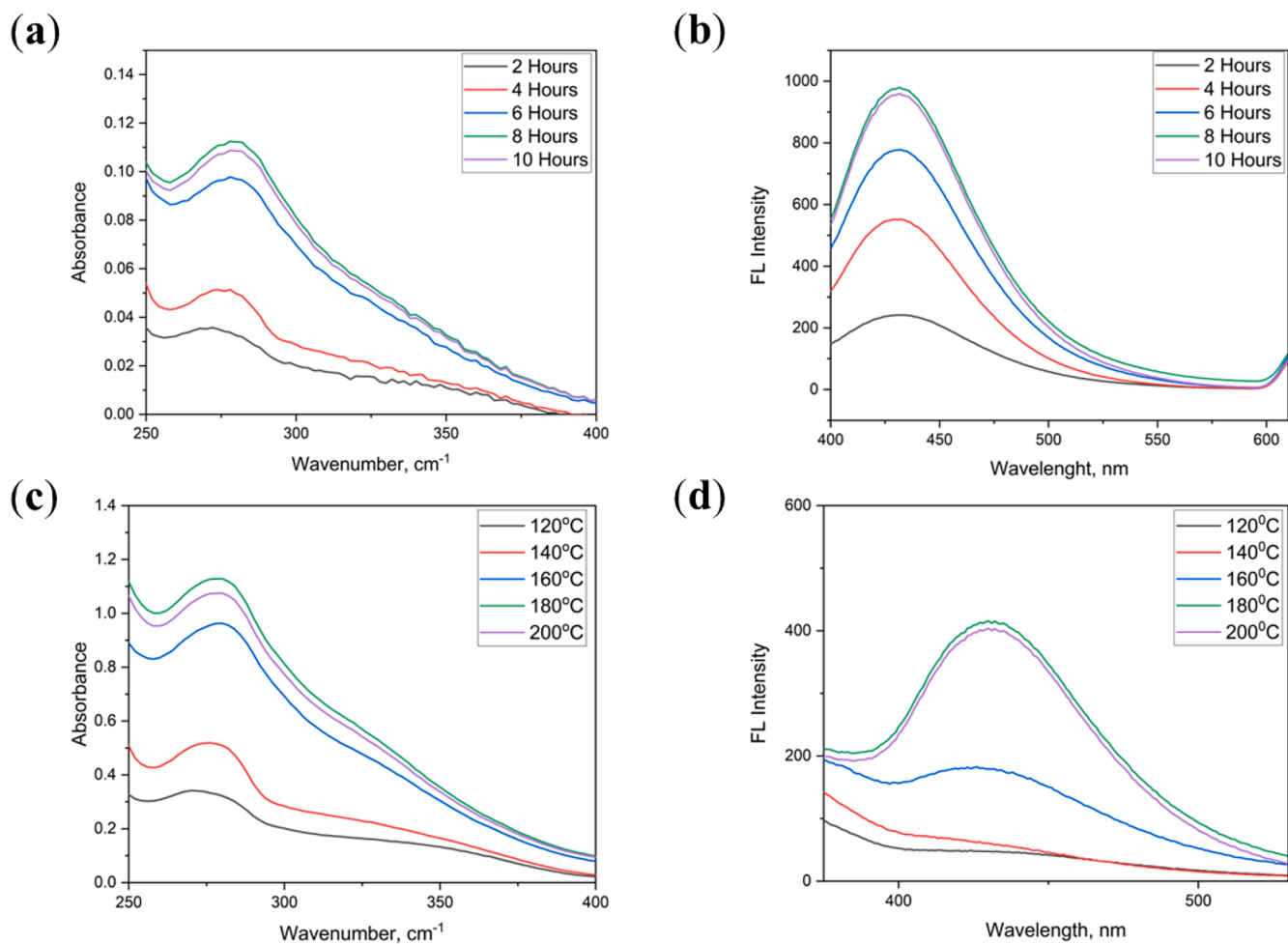


Fig. 5. Effect of N-CDs synthesis time (2–10 h) on UV–Visible absorption (a) and fluorescence spectra (b); Effect of N-CDs synthesis temperature (120–200 °C) on UV–Visible absorption spectra (c) and fluorescence spectra (d).

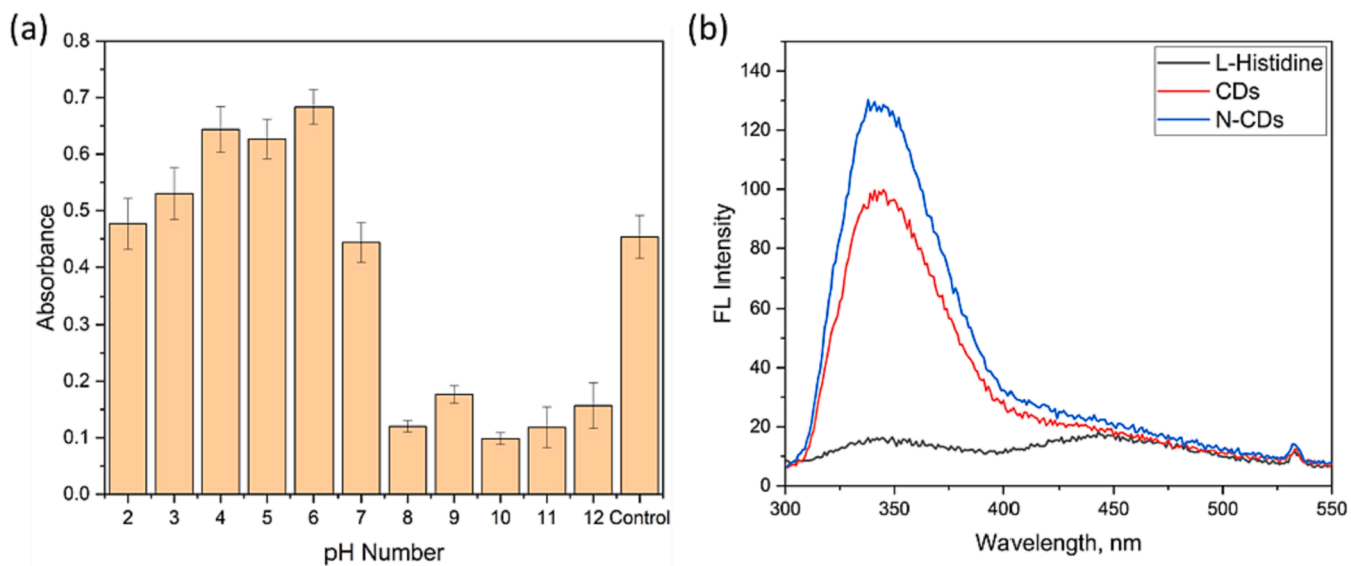

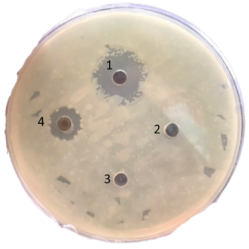

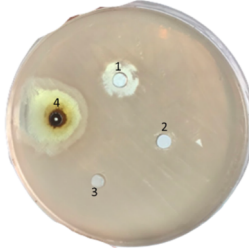


Fig. 6. (a) Effect of solution pH (2–12) on fluorescence intensity of N-CDs. (b) the enhanced fluorescence intensity of the N-CDs compared with bare CDs. * Error bars represent standard deviations of three independent measurements.

Table 3

Application of the obtained N-CDs for antimicrobial test by Agar disk diffusion assay.

Bacterial name	Inhibition zone of N-CDs	Positive/Negative test on Agar disk diffusion assay
<i>Escherichia coli</i>		1 = Amoxicillin, ++ 2 = DI water, - 3 = Ethanol 70 %, - 4 = N-CDs, ++
<i>Serratia marcescens</i>		1 = Amoxicillin, ++ 2 = DI water, - 3 = Ethanol 70 %, - 4 = N-CDs, +
<i>Bacillus megaterium</i>		1 = Amoxicillin, ++ 2 = DI water, - 3 = Ethanol 70 %, - 4 = N-CDs, +
<i>Staphylococcus aureus</i>		1 = Amoxicillin, ++ 2 = DI water, - 3 = Ethanol 70 %, - 4 = N-CDs, +++

water, and then one-pot synthesized using hydrothermal method in the optimum condition (180 °C, with 8 h).

2.4. Fluorescent N-CDs powder preparation

After get the optimum conditions of the N-CDs product, 5 g of the commercial tapioca flour powder was mixed with 20 mL N-CDs for 24 h at room temperature (Laboratory of Forensic Science, Khon Kaen University). The mixture was magnetically stirred at 400 rpm, kept dry in a 75 °C for 24 h in the oven to become powder. The powder was ground

using mortar and filter with laboratory test sieve with aperture 500 µm, after that the powder was kept at room temperature.

2.5. Latent fingerprints detection

The latent fingerprint was detected by using brushing method. The author touches the greasy area on his cheek or forehead, and the fingerprint printed on the different non-porous material surfaces for 5 s (aluminum foil, glass and plastic). For the latent fingerprint detection, the N-CDs/Starch powder was brushed on the fingerprint. Then, the latent fingerprint was detected.

2.6. Antibacterial test

The bacteria (*Escherichia coli*, *Serratia marcescens*, *Bacillus megaterium* and *Staphylococcus aureus*) were inoculated from an inclined medium and cultured by using 0.5 McFarland Methods at 37 °C and for 24 h. Finally, 1.5×10^8 CFU/mL of bacterial suspension was obtained for use.

The N-CDs sample was tested using agar plate assay. 3 g of medium agar was diluted with 100 mL DI water and sterilized by autoclave. After the agar medium was prepared, swab 3D dimensional of each bacteria stain to the media agar from the stock (1.5×10^8 CFU/mL), and the N-CDs with concentration 25 % (%wt/v) results were compared with those of control plates using DI water, alcohol 96 % and commercial amoxicillin drug concentration 25 % (%wt/v).

2.7. Presto blue assay

The cells culture of human gingival fibroblast (HGF) used for testing were human gum fiber-forming cells grown in a 75-cubic centimeter cell culture flask, with DMEM cell culture medium (DMEM; Dulbecco's Modified Eagles, Gibco, USA) containing 10 % fetal bovine serum and incubated in an incubator with temperature of 37 °C (Sheldon, USA) under 5 % carbon dioxide gas and 95 % relative humidity. Cells are grown until they look like single-layer cells. When testing the cells, suck the cell culture medium out of the flask with 2 mL phosphate buffer saline (PBS). Suck off the phosphate buffer saline from the cell culture flask. Then trypsin-EDTA 0.25 %, 2 mL was added, leave for 3 min, place the cell culture flask into the incubator, etc. When the time is up, add DMEM cell culture medium containing 10 % fetal bovine serum 2 mL, aspirate 10 µL of cell solution, and place it into a microtube. Add 10 µL of 0.4 % trypan blue stain (Gibco, USA) and mix well. Take 10 µL of the mixture and put it in an automatic cell counter (TC20TM Automated Cell Counter) (Bio Rad, USA) to adjust to get 1×10^5 cells/mL. For the measurement of the viability of gill filament cells using the Presto blue assay, add 1×10^4 cells in each well of a 96-well plate and keeping them in a controlled incubator with 5 % carbon dioxide gas helped find out how harmful the substances were to human gum filament cells. At a temperature of 37 °C and a relative humidity of 95 % for 24 h, vacuum up all the old cell culture media. Add the substance to be tested, concentrations of 0.1, 0.15 and 0.2 mg/L, and add the DMEM cell culture medium with 10 % fetal bovine serum in the positive control group and 10 % dimethyl sulfoxide solution (DMSO, Merck, Germany) added as the negative control group (negative control). Continue to culture cells for 72 h. After 72 h, suck out all the old cell culture media. Add 100 µL of Presto blue solution to each well, place it in the incubator for 45 min, and then measure the fluorescence of the Presto blue solution. Using a microplate reader (Microplate Reader, Varioskan LUX, Thermo Fisher Scientific) with an excitation wavelength of 560 nm and an emission wavelength of 590 nm, and calculating the average percentage of cell life; Percentage of cell viability = (mean fluorescence value of sample at various concentrations/mean fluorescence value of positive control) × 100.

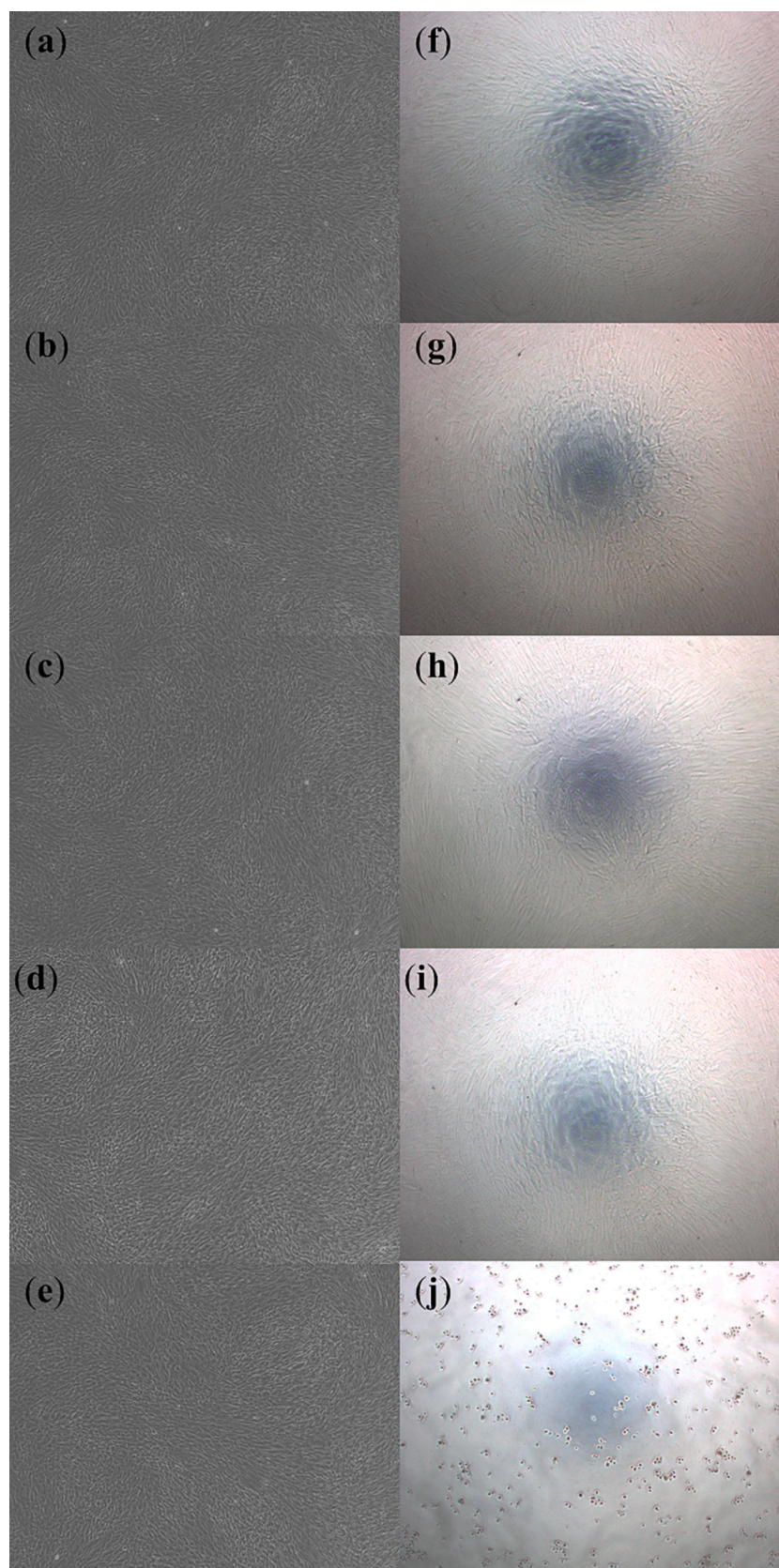


Fig. 7. Presto blue assay for human gingival fibroblast test before 72 h with various concentrations of N-CDs: (a) 0.1 mg/L, (b) 0.15 mg/L, (c) 0.2 mg/L, (d) positive control, and (e) negative control, and after 72 h with various concentrations of N-CDs: (f) 0.1 mg/L, (g) 0.15 mg/L, (h) 0.2 mg/L, (i) positive control and (j) negative control. (For interpretation of the references to color in this figure legend, the reader is referred to the web version of this article.)

Table 4
Total phenolic content and antioxidant activity of the N-CDs sample.

Sample	Total phenolic content (mg GAE/g)	Antioxidant activity	
		IC ₅₀ by DPPH (mg/L)	IC ₅₀ by ABTS (mg/L)
N-CDs	1,480.89 ± 16.78	6.38 ± 1.30	8.57 ± 2.53

Table 5
Comparison Antioxidant by DPPH Lc50.

Sample	Antioxidant activity IC50 by DPPH (mg/L)	
N-CDs	6.38 ± 1.30	This Work
Coconut CDs	0.06	(Chunduri et al., 2017)
Ginger essential oil	11.6	(Eissa et al., 2010)
GCDs	0.175	(Murru et al., 2020)
Shell CDs	0.025	(Li et al., 2017)

2.8. Antioxidant activity by ABTS and DPPH methods

Various concentrations of N-were prepared as 0, 5, 10, 20, 30, 40, and 50 µg/mL in a 99 % ethanol solvent, mix with 80 µL of ABTS, and add 580 µL of phosphate buffer and mix well together in 96-well plate set in the dark for 20 min, and then measure the absorbance at 734 nm, and calculating by % Inhibiting effect = $(\text{Absorbance}_{\text{Control}} - \text{Absorbance}_{\text{Sample}} / \text{Absorbance}_{\text{Control}}) \times 100$.

In addition, 60 µg/mL of DPPH solution was mixed into 99 % ethanol, then prepared the N-CDs in the various concentrations of 0, 5, 10, 20, 30, 40, and 50 µg/mL in 99 % ethanol solvent, added the various amounts of N-CDs and DPPH solution into the tube and left in the dark for 20 min. After that, the absorbance was measured with a UV-Vis Spectrophotometer. At a wavelength of 517 nm, % Scavenging =

$$(\text{Absorbance}_{\text{Control}} - \text{Absorbance}_{\text{Sample}} / \text{Absorbance}_{\text{Control}}) \times 100.$$

3. Results and discussion

3.1. Morphology images by TEM & FIB-SEM and elemental component by EDX of N-CDs

The diameter of the N-CDs nanoparticle was measured by TEM and it was found that the particle size of N-CDs is around 4 nm (Fig. 2a and Fig. 2b). Fig. 2c shows that when CDs doped with L-histidine, the CDs are likely functionalized with the L-histidine. The elemental component of N-CDs was scanned using energy dispersive X-ray (EDX) spectrum as shown in Fig. 2d, the elemental composition of the N-CDs contains mainly for C 71.8 % and O 24.8 %. the N atom is not detected in this EDX because N lacks a K shell, except in covalent relationships where it possesses a K shell that is exclusively shared by the involved electrons.

3.2. FTIR characteristics of N-CDs

The functional groups of N-CDs were identified by FTIR. In Fig. 3a it is shown that N-CDs consist of O—H bond stretching at 3300 cm⁻¹, 2920 cm⁻¹ for alkane bonding (C—H), C=O bonding strongly appears at 1700 cm⁻¹, C—O stretching can be found at 1194 cm⁻¹, 1022 cm⁻¹, and 774 cm⁻¹ was of CH₂ stretching bonds. Fig. 3b shows the characteristic of CDs from *Zingiber Montanum* with starch sample and it also contains the O—H stretching at 3300 cm⁻¹, the C—H stretching for alkene at 2900 cm⁻¹, 1650 cm⁻¹ and 1000 cm⁻¹. At 1319 cm⁻¹ presents the bending of C-CHO aldehyde (Fàbrega et al., 2018; Liu et al., 2018).

Table 6
Application of the N-CDs/Starch powder compared with CDs/Starch powder for latent fingerprint detection on glass, plastic and aluminum visualized under visible lamp and UV lamp.








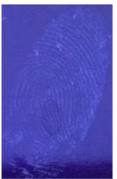




Material type	Visible lamp (N-CDs)	UV lamp (N-CDs)	Visible lamp (CDs)	UV lamp (CDs)
Glass				
Plastic				
Aluminum				




Table 7

The impact of storage duration and temperature on the efficacy of latent fingerprint development using the N-CDs/Starch powder on various non-porous surface substrates.

Material type	Day period	60 °C	- 4 °C	Room temp.
Plastic	7	/	/	//
	14	/	/	//
	21	/	/	//
	28	/	/	//
Glass	7	//	/	//
	14	//	/	//
	21	/	/	//
	28	/	/	//
Iron	7	//	/	//
	14	//	/	//
	21	/	/	//
	28	/	/	//
Aluminum	7	//	/	//
	14	//	/	//
	21	//	/	//
	28	/	/	//
Varnished wood	7	//	/	//
	14	//	/	//
	21	//	/	//
	28	//	/	//
Note: /	Detected			
//	Minutiae detected			

Table 8

Durability test of latent fingerprint detection using the developed N-CDs/Starch powder with various duration times.



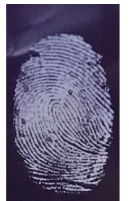
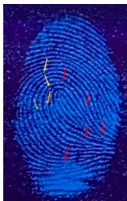
Material type	1st Day	30th Day	90th Day
Glass			

3.3. Elemental analysis of N-CDs using XPS and CHN analyzer

The chemical details of CDs and N-CDs were investigated by using X-ray photoelectron spectroscopy as shown in Fig. 4. The N-CDs (Fig. 4 a) spectra show the element of Cs1 on 285 eV, Ns1 on 399 eV and Os1 on 531 eV. Fig. 4 also shows the peaks for Cs1 at 284.8 eV and 283.3 eV which are related to C=C, and C-C (Fig. 4b). and the peaks for O1s on 529.3 eV, C=O 530.5 eV and 531.1 eV (Fig. 4c), and show the N1s peaks on 399 eV (Liu et al., 2019; Liu et al., 2017; Nugroho et al., 2023; Ganguly et al., 2020; Luo et al., 2020), CDs spectra show the element of

Table 9

Latent fingerprint detection using N-CDs/starch powder compared with the commercial powder visualized under both normal lamp and UV lamp.

Material type	Commercial powder (Normal lamp)	Commercial powder (UV lamp)	N-CDs/Starch (Normal lamp)	N-CDs/Starch (UV lamp)
Glass				

C1s and O1s (284. And 532.08 eV) were shown in the Fig. 4e. the peaks for Cs1 at 284.7 eV, and 285.9 eV, which are related to C—O—C, and C—O, (Fig. 4f). and the peaks for O1s on 532.2 eV, O—C. 533.3 eV represent of C—OH and 534.8 eV is C—O (Fig. 4g), respectively (Li et al., 2018; Chen et al., 2017; Liu et al., 2018). In this study, the elemental analysis of both CDs and N-CDs was analyzed using CHNS analyzer as reported in the Table 2, particularly the N element was found around 5.49 %.

3.4. Optical properties of N-CDs

N-CDs from *Zingiber Montanum* were preliminary analyzed by UV-Visible and fluorescence spectroscopy. The optical properties of this carbon dots were also visualized under commercial UV Lamp. The optimum conditions of N-CDs were synthesized under various times as 2 h, 4 h, 6 h, and 8 h and various temperatures as 120 °C, 140 °C, 160 °C, and 180 °C by using hydrothermal method. Fig. 5 shows those results after their synthesis procedure of N-CDs with various conditions, and analyzed by a UV-Visible and fluorescence spectrophotometer. Fig. 5a shows that the N-CDs product from 8 h gave a more optimum absorbance (UV-Vis) than other data, as well as their fluorescence intensity. Fig. 5b, at the same time, the comparison with temperature variation conditions can be seen in Fig. 5c. and 5d. It was evident that the synthesized N-CDs had a high peak emission wavelength at 445 nm with excitation wavelength 380 nm, via the synthesis condition temperature at 180 °C. It is shown to have an intensity and absorbance higher than others. Thus, in this case the optimum data was obtained from this synthetic route.

The effect of solution pH also investigated in details. The 50 µL N-CDs was mixed into 1 mL buffer solution pH range from 2 to 12, then adjusted to 10 mL using DI water. The result is shown in Fig. 6(a). At acid range its effect to increase the fluorescence intensity of the N-CDs, it was found that pH 2 until pH 6 give the fluorescence intensity higher than control. In addition, pH 7 to pH 12 make the intensity of N-CDs is lower than standard control, so the optimum condition is around pH 6. Fig. 6 (b) shows that L-histidine can enhance the intensity of CDs because of the N atom in the L-histidine structure, Nitrogen doping may induce quantum confinement effects in carbon dots, especially if the nitrogen atoms are strategically placed in specific regions of the carbon dot structure. Quantum confinement can lead to discrete energy levels and size-dependent electronic properties, influencing the emission characteristics. The quantum yield of N-CDs was also calculated by using a |e-UV-Vis-IR Spectral Software, and it is shown the N-CDs has its quantum yield of 16 % (Wu et al., 2014; Fletcher, 1969).

3.5. Antibacterial and antioxidant activities of the N-CDs

The N-CDs were applied for antimicrobial test by agar diffusion assay using various gram-negative bacterial and gram-positive bacteria including *Escherichia coli*, *Serratia marcescens*, *Bacillus megaterium* and *Staphylococcus aureus* as shown in Table 3 (Liang et al., 2021; Qie et al., 2022). The effect of antimicrobial activity against both *E. coli* and

B. megaterium (N-CDs #4 plate) have a similar clear zone with the amoxicillin as a standard control. For *S. marcescens*, it is shown that its clear zone of amoxicillin is wider than that of N-CDs, but the N-CDs can still be found to use for antimicrobial activity. In this study, the N-CDs show a good potential antimicrobial activity for *Staphylococcus aureus* because the clear zone is wider than control, it would be recognized, for both *in vitro* and *in vivo*, the N-CDs are typically regarded as benign and harmless substances. The N-doped carbon dots will have its ability to interact with the bacterial cell membrane as usual, resulting in physical and mechanical damage through two distinct mechanisms. Firstly, electrostatic interactions facilitate surface adherence, allowing the carbon dots to bind to the bacterial cell membrane. Secondly, the carbon dots disrupt the bacterial cell wall, further contributing to the inflicted damage. The disruption and penetration of the bacterial cell membrane, the induction of oxidative stress with damages to DNA/RNA, leading to the alteration or inhibition of key gene expressions, and the induction of oxidative damages to proteins and other intracellular biomolecules are all components of the action mechanism. The N-CDs adhere to the bacterial surface and produce reactive oxygen species (ROS), which are known to inhibit microorganisms (Al Awak et al., 2017; Li et al., 2018; Li et al., 2016; Ge et al., 2016; Ipe et al., 2005).

In addition, cytotoxicity trial was also performed using various concentrations of N-CDs (ranging from 0.1 to 0.2 mg/L) on multiple samples, and the responses of human gingival fibroblast (HGF) cells were assessed using the presto blue assay. According to the data presented in Fig. 7, the viability of HGF cells remained unaffected after being treated with various compositions of N-CDs for a duration of 72 h, specifically at doses of 0.1 and 0.15 mg/L. At elevated doses, the viability of the cells exhibited a dose-dependent drop, resulting in a reduction of cell viability to 78 % at a dosage of 0.2 mg/L. For the remaining concentrations, the cell viability was approximately 99 % at a concentration of 0.1 mg/L and approximately 96 % at a concentration of 0.15 mg/L. The findings of this study indicate that in order to prevent cellular toxicity, it is advisable to employ N-CDs at concentrations not exceeding 0.15 mg/L.

Besides, the antioxidant *in vitro* study of N-CDs at different concentrations according to two standard methods. Free radical scavenging effect of N-CDs using the DPPH method was $LC_{50} 6.38 \pm 1.30$ mg/L. Inhibiting activity of free radicals with N-CDs using the ABTS method gave an $LC_{50} 8.57 \pm 2.53$ mg/L. This antioxidant study of the N-CDs is then acting to eliminate free radicals or the effect of reducing heavy metal ions. That is often related due to the total phenolics found in rather high amounts of 1480.89 ± 16.78 mg GAE/g DW (Table 4). Compare with others Carbon Dots from natural resources, the N-CDs show higher antioxidant activities in the DPPH assay methods compare the others CDs, but lower compare the ginger essential oil (Table 5).

3.6. Latent fingerprint detection on-nonporous surface materials using N-CDs

For latent fingerprint detection, the fine powder of N-CDs/starch was prepared, and then was brushed on the non-porous surface materials by brushing method. Both N-CDs/starch and CDs/starch powder were brushed on glass, ceramic, aluminum and coaster, and their latent fingerprints were detected under UV lamp (365 nm) and visible lamp. Table 6 shows the latent fingerprint detection on those materials. It was shown that the N-CDs/starch powder gives more brightness and marks more details of minutiae compared with bare CDs/starch. For the effect of storage time at different temperatures, a volunteer presses the fingerprint on those material surfaces (plastic, iron, glass, aluminum and varnish wood) as well. The material was kept at room temperature, at -4 °C and at 60 °C. Various surface materials were dried in the oven with temperature a 60 °C for 30 min before applied with the N-CDs/starch powder. Table 7 shows that the N-CDs/starch can be used to detect the latent fingerprint on many material surfaces, especially at room temperature, with the symbol of // meaning that the powder can use to

detect the minutiae of the latent fingerprint, and / meaning that the powder can detect the latent fingerprint but that the minutiae cannot be clear. The durability and resistance of the N-CDs/starch powder were also studied, in this regard, the fine powder was compared during the day prepared 30-day, and 90-day, under the condition that the powder was kept at room temperature. Table 8 shows that the N-CDs/starch powder can be used for latent fingerprint detection on these surfaces, either the result is not so clear as the first time.

Furthermore, this study was aimed to investigate the comparison between the detection of latent fingerprints on non-porous material surfaces by a volunteer who imprinted his index finger, and the use of commercial black powder. The surface material was coated with N-CDs detection powder and subsequently examined under using both an LED lamp and a UV lamp with a wavelength of 365 nm. Table 9 presents the comparative analysis of the latent fingerprint detection on those surface materials, specifically focusing on glass surface. The utilisation of the N-CDs enhances the visibility of fingerprints when examined under UV lamp, enabling the detection of a greater number of minutiae. Conversely, the use of commercial powder yields clearer results when observed under a normal lamp, with distinct color coding representing different features of the fingerprint (red for bifurcation, yellow for termination, green for island, and orange for lake).

4. Conclusion

The addition of L-histidine enhances the fluorescence intensity of carbon dots derived from *Zingiber Montanum* extract. The N-CDs' particle size, as determined by transmission electron microscopy (TEM), was around 4 nm. Additionally, the presence of C-N linkages was confirmed by XPS analysis. The N-CDs were utilised in their applications for detecting latent fingerprints on different non-porous surface materials. The study demonstrates that N-CDs/starch powder may effectively identify latent fingerprints on a range of surfaces, including plastic, aluminium, and glass. This study also examined the impact of temperature and storage duration on the accuracy of minutiae detection. The storage time of N-CDs/starch powder was tested for a period of 28 days, and the durability of the powder was evaluated for latent fingerprint detection over a span of 90 days. Furthermore, the N-CDs were evaluated for their antibacterial properties against several types of gram-negative and gram-positive bacteria, such as *Escherichia coli*, *Serratia marcescens*, *Bacillus megaterium*, and *Staphylococcus aureus*. The results demonstrated that the N-CDs had the potential to be used as an effective antimicrobial agent.

Author Contributions: all authors are contributed in this research.

Acknowledgments

1. Research Center for Environmental and Hazardous Substance Management (EHSM), Khon Kaen University; 2. Materials Chemistry Research Center (MCRC), Department of Chemistry, Faculty of Science, and Center of Excellence for Innovation in Chemistry (PERCH-CIC). 3. SUT-NANOTEC-SLRI beamline, Synchrotron Light Research Institute, Thailand for XPS analysis. 4. Graduated school Khon Kaen University, for the financial support.

References

- Abdel Maksoud, M.I.A., Ghobashy, M.M., Kodous, A.S., Fahim, R.A., Osman, A.I., Al-Muhtaseb, A.A.H., Ashour, A.H., 2022. Insights on magnetic spinel ferrites for targeted drug delivery and hyperthermia applications. *Nanotechnol. Rev.* 11 (1), 372–413.
- Al Awak, M.M., Wang, P., Wang, S.Y., Tang, Y.A., Sun, Y.P., Yang, L.J., 2017. Correlation of carbon dots' light-activated antimicrobial activities and fluorescence quantum yield. *Rsc Adv.* 7, 30177–30184.
- Alam, A.-M., Park, B.-Y., Ghouri, Z.K., Park, M., Kim, H.-Y., 2015. Synthesis of Carbon Quantum Dot from Cabbage with Down- and Up-Conversion Photoluminescence Properties: Excellent Imaging Agent for Biomedical Application. *Green Chem.* 17, 3791–3797.

- Allianou, N., Stratigou, T., Christodoulatos, G.S., Dalamaga, M., 2019. Understanding the Role of the Gut Microbiome and Microbial Metabolites in Obesity and Obesity-Associated Metabolic Disorders: Current Evidence and Perspectives. *Curr. Obes. Rep.* 8, 317–332.
- Alshangiti, D. M., Ghobashy, M. M., Alkhursani, S. A., Shokr, F. S., Al-Gahtany, S. A., & Madani, M. M. (2019). Semi-permeable membrane fabricated from organoclay/PS/EVA irradiated by γ -rays for water purification from dyes. *J. Mater. Res. Technol.* 2019, 8(6), 6134–6145.
- Bhalla, N., Jolly, P., Formisano, N., Estrela, P., 2016. Introduction to biosensors. *Essays Biochem.* 60, 1–8.
- Bilinski, P., Kapka-Skrzypczak, L., Posobkiewicz, M., Bondaryk, M., Holownia, P., Wojtyła, A., 2012. Public health hazards in Poland posed by foodstuffs contaminated with *E. coli* O104:H4 bacterium from the recent European outbreak. *Ann. Agric. Environ. Med.* 19, 3–10.
- Bramhanwade, K., Shende, S., Bonde, S., Gade, A., Rai, M., 2016. Fungicidal activity of Cu nanoparticles against *Fusarium* causing crop diseases. *Environ. Chem. Lett.* 14, 229–235.
- Chandrajith, V., Marapana, R., 2018. Physicochemical characters of bark exudates of *Lannea coromandelica* and its application as a natural fruit coating. *J. Pharmacogn. Phytochem.* 7, 1798–1802.
- Chen, S., Liu, M.-X., Yu, Y.-L., Wang, J.-H., 2019. Room-temperature synthesis of fluorescent carbon-based nanoparticles and their application in multidimensional sensing. *Sens. Actuators B Chem.* 288, 749–756.
- Chen, Y., Wang, H., Dang, B., Xiong, Y., Yao, Q., Wang, C., Jin, C., 2017. Bio-Inspired nacre-like nanolignocellulose-poly (vinyl alcohol)-TiO₂ composite with superior mechanical and photocatalytic properties. *Scientific Reports* 7 (1), 1823.
- Choi, C.A., Mazrad, Z.A., Lee, G., In, I., Lee, K.D., Park, S.Y., 2018. Boronate-based fluorescent carbon dot for rapid and selectively bacterial sensing by luminescence off/on system. *J. Pharm. Biomed. Anal.* 159, 1–10.
- Chunduri, L.A., Kurdekar, A., Patnaik, S., Rajasekhar, A.S., Prathibha, C., Kamiseti, V., 2017. Single Step Synthesis of Carbon Quantum Dots from Coconut Shell: Evaluation for Antioxidant Efficacy and Hemotoxicity. *J. Mater. Sci. Appl.* 3, 83–93.
- Dager, A., Uchida, T., Maekawa, T., Tachibana, M., 2019. Synthesis and characterization of Mono-disperse Carbon Quantum Dots from Fennel Seeds: Photoluminescence analysis using Machine Learning. *Sci. Rep.* 9, 14004.
- Diao, H., Li, T., Zhang, R., Kang, Y., Liu, W., Cui, Y., Wei, S., Wang, N., Li, L., Wang, H., et al., 2018. Facile and green synthesis of fluorescent carbon dots with tunable emission for sensors and cells imaging. *Spectrochim. Acta—Part A Mol.* 200, 226–234.
- Djunaidi, M.C., 2020. Gold imprinted adsorption based on eugenol. *IOP Publ.* 1524, 012077.
- Du, W., Xu, X., Hao, H., Liu, R., Zhang, D., Gao, F., Lu, Q., 2015. Green synthesis of fluorescent carbon quantum dots and carbon spheres from pericarp. *Sci. China Chem.* 58, 863–870.
- Du, F., Zeng, F., Ming, Y., Wu, S., 2013. Carbon dots-based fluorescent probes for sensitive and selective detection of iodide. *Microchim. Acta* 180, 453–460.
- Eissa, E.A., Basta, J.S., Ibrahim, V., 2010. The Oxidation Stability of Lubricating Oil. *Pet. Sci. Technol.* 28, 1611–1619.
- Fàbrega, C., Casals, O., Hernández-Ramírez, F., Prades, J.D., 2018. A review on efficient self-heating in nanowire sensors: Prospects for very-low power devices. *Sens. Actuators B Chem.* 256, 797–811.
- Fletcher, A.N., 1969. Quinine Sulfate As A Fluorescence Quantum Yield Standard. *Photochem. Photobiol.* 1969 (9), 439–444.
- Ganguly, S., Das, P., Itzhaki, E., Hadad, E., Gedanken, A., Margel, S., 2020. Microwave-Synthesized Polysaccharide-Derived Carbon Dots as Therapeutic Cargoes and Toughening Agents for Elastomeric Gels. *ACS Appl. Mater. Interfaces* 12, 51940–51951.
- Ge, J.C., Jia, Q.Y., Liu, W.M., Lan, M.H., Zhou, B.J., Guo, L., et al., 2016. Carbon Dots with Intrinsic Theranostic Properties for Bioimaging, Red-Light-Triggered Photodynamic/Photothermal Simultaneous Therapy In vitro and In vivo. *Adv Healthc Mater.* 5, 665–675.
- Gerc, A.J., Stanley-Wall, N.R., Coulthurst, S.J., 2014. Role of the phosphotransferase enzyme, PswP, in the biosynthesis of antimicrobial secondary metabolites by *Serratia marcescens* Db10. *Microbiology.* 160, 1609–1617.
- Ghobashy, M.M., Elhady, M.A., 2017. Radiation crosslinked magnetized wax (PE/Fe₃O₄) nano composite for selective oil adsorption. *Compos. Commun.* 3, 18–22.
- Ghobashy, M.M., Khafaga, M.R., 2017. Chemical modification of nano polyacrylonitrile prepared by emulsion polymerization induced by gamma radiation and their use for removal of some metal ions. *J. Polym Environ* 25, 343–348.
- Guan, W., Gu, W., Ye, L., Guo, C., Su, S., Xu, P., Ye, L., 2014. Microwave-assisted polyol synthesis of carbon nitride dots from folic acid for cell imaging. *Int. J. Nanomed.* 9, 5071–5078.
- Hashemi, N., Mousazadeh, M.H., 2021. Green synthesis of photoluminescent carbon dots derived from red beetroot as a selective probe for Pd²⁺ detection. *J. Photochem. Photobiol. A Chem.* 421, 113534.
- Hoozemans, J., de Brauw, M., Nieuwdorp, M., Gerdes, V., 2021. Gut Microbiome and Metabolites in Patients with NAFLD and after Bariatric Surgery: A Comprehensive Review. *Metabolites* 11, 353.
- Hu, Z., Jiao, X.-Y., Xu, L., 2020. The N, S co-doped carbon dots with excellent luminescent properties from green tea leaf residue and its sensing of gefitinib. *Microchem. J.* 154, 104588.
- Ipe, B.I., Lehnig, M., Niemeyer, C.M., 2005. On the generation of free radical species from quantum dots. *Small.* 1, 706–709.
- Jayan, S.S., Jayan, J.S., Sneha, B., Abha, K., 2021. Facile synthesis of carbon dots using tender coconut water for the fluorescence detection of heavy metal ions. *Mater. Today Proc.* 43, 3821–3825.
- Jiao, Y., Gong, X., Han, H., Gao, Y., Lu, W., Liu, Y., Xian, M., Shuang, S., Dong, C., 2018. Facile synthesis of orange fluorescence 1 carbon dots with excitation independent emission for pH sensing and cellular imaging. *Anal. Chim. Acta* 1042, 125–132.
- Kaper, J.B., Nataro, J.P., Mobley, H.L., 2004. Pathogenic *Escherichia coli*. *Nat. Rev. Microbiol.* 2, 123–140.
- Kaur, N., Singh, M., Moumen, A., Duina, G., Comini, E., 2020. 1D Titanium Dioxide: Achievements in Chemical Sensing. *Material* 13, 2974.
- Koutsogiannis, P., Thomou, E., Stamatis, H., Gournis, D., Rudolf, P., 2020. Advances in fluorescent carbon dots for biomedical applications. *Adv. Phys.-X* 5, 1758592.
- Li, J., Fu, W., Zhang, X., Zhang, Q., Ma, D., Wang, Y., Zhu, D., 2023. Green preparation of ginger-derived carbon dots accelerates wound healing. *Carbon* 208–215.
- Li, Y.J., Harroun, S.G., Su, Y.C., Huang, C.F., Unnikrishnan, B., Lin, H.J., et al., 2016. Synthesis of Self-Assembled Spermidine-Carbon Quantum Dots Effective against Multidrug-Resistant Bacteria. *Adv Healthc Mater.* 5, 2545–2554.
- Li, H., Huang, J., Song, Y.X., Zhang, M.L., Wang, H.B., Lu, F., et al., 2018. Degradable Carbon Dots with Broad-Spectrum Antibacterial Activity. *ACS Appl Mater Inter.* 10, 26936–26946.
- Li, F., Li, T., Sun, C., Xia, J., Jiao, Y., Xu, H., 2017. Selenium-Doped Carbon Quantum Dots for Free-Radical Scavenging. *Angew. Chem.* 129, 9910–9914.
- Li, C.-L., Ou, C.-M., Huang, C.-C., Wu, W.-C., Chen, Y.-P., Lin, T.-E., Chang, H.-T., 2014. Carbon dots prepared from ginger exhibiting efficient inhibition of human hepatocellular carcinoma cells. *J. Mater. Chem. B* 2 (28), 4564.
- Li, X.C., She, F.S., Shen, D., Liu, C.P., Chen, L.H., Li, Y., Wang, H.E., 2018. Coherent nanoscale cobalt/cobalt oxide heterostructures embedded in porous carbon for the oxygen reduction reaction. *RSC Advances* 8 (50), 28625–28631.
- Liang, J., Li, W., Chen, J., Huang, X., Liu, Y., Zhang, X., Zhang, H., 2021. Antibacterial Activity and Synergetic Mechanism of Carbon Dots against Gram-Positive and -Negative Bacteria. *ACS Appl. Bio Mater.* 9, 6937–6945.
- Liu, Q., Chen, C., Du, M., Wu, Y., Ren, C., Ding, K., Huang, C., 2018. Porous hexagonal boron nitride sheets: effect of hydroxyl and secondary amino groups on photocatalytic hydrogen evolution. *ACS Applied Nano Materials* 1 (9), 4566–4575.
- Liu, Y., Jiang, L., Li, B., Fan, X., Wang, W., Liu, P., Xu, S., Luo, X., 2019. Nitrogen doped carbon dots: Mechanism investigation and their application for label free CA125 analysis. *J. Mater. Chem. B* 10, 1039.
- Liu, X., Liu, J., Zheng, B., Yan, L., Dai, J., Zhuang, Z., Du, J., Guo, Y., Xiao, D., 2017. N-doped carbon dots: Green and efficient synthesis on large-scale and their application in fluorescent pH sensing. *New J. Chem.* 41, 10607–10612.
- Lu, S., Guo, S., Xu, P., Li, X., Zhao, Y., Gu, W., Xue, M., 2016. Hydrothermal synthesis of nitrogen-doped carbon dots with real-time live-cell imaging and blood-brain barrier penetration capabilities. *Int. J. Nanomed.* 11, 6235–6336.
- Luo, H., Dimitrov, S., Daboczi, M.; Kim, J.-S.; Guo, Q.; Fang, Y.; Stoeckel, M.-A.; Samorì, P.; Fenwick, O.; Sobrido, A.B.J.; et al. Nitrogen-Doped Carbon Dots/TiO₂ Nanoparticle Composites for Photoelectrochemical Water Oxidation.(2020). *ACS Appl. Nano Mater.* 2020, 3, 3371–3381.
- Macairan, J.-R., Jaunky, D.B., Naccache, R., Piekny, A., 2019. Intracellular ratiometric temperature sensing using fluorescent carbon dots. *Nanoscale Adv.* 1, 105–113.
- Murru, C., Badía-Laíño, R., Díaz-García, M.E., 2020. Synthesis and characterization of green carbon dots for scavenging radical oxygen species in aqueous and oil samples. *Antioxidants.* 9 (11), 1147.
- Naik, G.G., Alam, M.B., Pandey, V., Dubey, P.K., Parmar, A., Sahu, A., 2020. Pink Fluorescent Carbon Dots Derived from the Phytomedicine for Breast Cancer Cell Imaging. *ChemistrySelect* 5, 6594–6960.
- Nugroho, D., Keaprom, C., Chanthai, S., Oh, W.-C., Benchawattananon, R., 2022. Highly Sensitive Fingerprint Detection under UV Light on Non Porous Surface Using Starch-Powder Based Luminol-Doped Carbon Dots (N-CDs) from Tender Coconut Water as a Green Carbon Source. *Nanomaterials* 12, 400.
- Nugroho, D., Oh, W.-C., Chanthai, S., Benchawattananon, R., 2022. Improving Minutiae Image of Latent Fingerprint Detection on Non-Porous Surface Materials under UV Light Using Sulfur Doped Carbon Quantum Dots from Magnolia Grandiflora Flower. *Nanomaterials.* 12, 3277.
- Nugroho, D., Chanthai, S., Oh, W.-C., Benchawattananon, R., 2023. Fluorophores-rich natural powder from selected medicinal plants for detection latent fingerprints and cyanide. *Science Progress.* 2023 (106), 1.
- Oldock, E., Surewaard, B.G.J., Shamarina, D., Na, M., Fei, Y., Ali, A., Williams, A., Pollitt, E.J.G., Szkuta, P., Morris, P., et al., 2018. Human skin commensals augment *Staphylococcus aureus* pathogenesis. *Nat. Microbiol.* 3, 881–890.
- Qie, X., Zan, M., Gui, P., Chen, H., Wang, J., Lin, K., Song, Y., 2022. Design, Synthesis, and Application of Carbon Dots With Synergistic Antibacterial Activity. *Front. Bioeng. Biotechnol.* 10.
- Rao, B., Zhang, L.Y., Sun, J., Su, G., Wei, D., Chu, J., Zhu, J., Shen, Y., 2012. Characterization and regulation of the 2,3-butenediol pathway in *Serratia marcescens*. *Appl. Microbiol. Biotechnol.* 93, 2147–2159.
- Roshni, V., Othoor, D., 2015. Synthesis of carbon nanoparticles using one step green approach and their application as mercuric ion sensor. *J. Lumin.* 161, 117–122.
- Sahu, S., Behera, B., Maiti, T.K., Mohapatra, S., 2012. Simple one-step synthesis of highly luminescent carbon dots from orange juice: Application as excellent bio-imaging agents. *Chem. Commun.* 48, 8835–8837.
- Srivastava, S., Bist, V., Srivastava, S., Singh, P.C., Trivedi, P.K., Asif, M.H., Chauhan, P.S., Nautiyal, C.S., 2016. Unraveling aspects of *Bacillus amyloliquefaciens* mediated enhanced production of rice under biotic stress of *Rhizoctonia solani*. *Front. Plant Sci.* 7, 587.
- Tang, M., Ren, G., Zhu, B., Yu, L., Liu, X., Chai, F., Wu, H., Wang, C., 2019. Facile synthesis of orange emissive carbon dots and their application for mercury ion detection and fast fingerprint development. *Anal. Methods* 11, 2072–2081.

- Vallianou, N., Liu, J., Dalamaga, M., 2019. What are the key points in the association between the gut microbiome and nonalcoholic fatty liver disease? *Metabol. Open* 1, 9–10.
- Wang, H., Sun, C., Chen, X., Zhang, Y., Colvin, V.L., Rice, Q., Seo, J., Feng, S., Wang, S., Yu, W.W., 2017. Excitation wavelength independent visible color emission of carbon dots. *Nanoscale* 9, 1909–1915.
- Wang, H., Mu, Q., Wang, K., Revia, R.A., Yen, C., Gu, X., Tian, B., Liu, J., Zhang, M., 2019. Nitrogen and boron dual-doped graphene quantum dots for near-infrared second window imaging and photothermal therapy. *Appl. Mater. Today* 14, 108–117.
- Williamson, N.R., Fineran, P.C., Leeper, F.J., Salmond, G.P., 2006. The biosynthesis and regulation of bacterial prodiginines. *Nat. Rev. Microbiol.* 4, 887–899.
- Wu, Z.L., Gao, M.X., Wang, T.T., Wan, X.Y., Zheng, L.L., Huang, C.Z., 2014. A general quantitative pH sensor developed with dicyandiamide N-doped high quantum yield graphene quantum dots. *Nanoscale* 6, 3868–3874.
- Xu, H., Yang, X., Li, G., Zhao, C., Liao, X., 2015. Green Synthesis of Fluorescent Carbon Dots for Selective Detection of Tartrazine in Food Samples. *J. Agric. Food Chem.* 63 (30), 6707–6714.
- Yang, T., Huang, J.-L., Wang, Y.-T., Zheng, A.-Q., Shu, Y., Wang, J.-H., 2019. β -cyclodextrin decorated carbon dots serve as nanocarrier for targeted drug delivery and controlled release. *ChemNanoMat* 5, 479–487.
- Yang, D., Li, J., Cheng, Y., Wan, F., Jia, R., Wang, Y., 2019. Compound repair effect of carbon dots and Fe²⁺ on iron deficiency in Cucumis melon L. *Plant Physiol. Biochem.* 142, 137–142.
- Yang, X., Zhang, B., Liu, Z., Deng, B., Yu, M., Li, L., Jiang, H., Li, J., 2011. Preparation of the antifouling microfiltration membranes from poly(N, N-dimethylacrylamide). *J. Mater. Chem.* 21, 11908.
- Ye, S.-L., Huang, J.-J., Luo, L., Fu, H.-J., Sun, Y.M., Shen, Y.-D., Lei, H.-T., Xu, Z.-L., 2017. Preparation of Carbon Dots and Their Application in Food Analysis as Signal Probe. *Chin. J. Anal. Chem.* 45, 1517–1581.
- Yong, J., Ge, L., Ng, Y.F., Tan, S.N., 2009. The Chemical Composition and Biological Properties of Coconut (Cocos nucifera L.) Water. *Molecules* 14, 5144–5164.
- Zhang, Q., Zhao, Q., Fu, M., Fan, X., Lu, H., Wang, H., Zhang, Y., Wang, H., 2018. Carbon quantum dots encapsulated in super small platinum nanocrystals core-shell architecture/nitrogen doped graphene hybrid nanocomposite for electrochemical biosensing of DNA damage biomarker-8'-hydroxy-2'-deoxyguanosine. *Anal. Chim. Acta* 1047, 9–20.